ELSEVIER

Surface Science 401 (1998) 371–391

surface science

Oxidation mechanism of propylene on an Ag surface: dipped adcluster model study

Zhen-Ming Hu [a], Hiromi Nakai [a,1], Hiroshi Nakatsuji [a,b,c,*]

[a] *Department of Synthetic Chemistry and Biological Chemistry, Graduate School of Engineering, Kyoto University, Sakyo-ku, Kyoto 606-01, Japan*

[b] *Department of Applied Chemistry, Graduate School of Engineering, The University of Tokyo, Hongo, Tokyo 113, Japan*

[c] *Institute for Fundamental Chemistry, 34-4 Takano-Nishihiraki-cho, Sakyo-ku, Kyoto 606, Japan*

Received 14 April 1997; accepted for publication 18 December 1997

Abstract

The mechanisms of the epoxidation and complete oxidation of propylene over a silver surface are studied by the dipped adcluster model (DAM) combined with the ab initio HF and MP2 methods. Several postulated reaction pathways involving both molecularly and atomically adsorbed oxygens are investigated. The energy diagrams of the epoxidation and complete oxidation of propylene on the silver surface are presented, and the detailed electronic mechanisms for the oxidation of propylene are clarified. The calculations show that the mechanism involving the single precursor intermediate common to both epoxidation and complete oxidation proposed in some literatures can be ruled out. Instead, the two competitive mechanisms are suggested: the epoxide formation is initiated by the reaction of the olefinic carbon with the adsorbed oxygen, while the combustion is initiated by the abstraction of the allylic hydrogen by the adsorbed oxygen. The former mechanism is essentially the same as that in the epoxidation of ethylene reported previously. The latter mechanism is energetically more favorable for propylene, which is a reason for the low selectivity of the epoxidation of propylene. The adsorbed allyl species, which is an intermediate in the latter mechanism, is demonstrated to exist in the form of chemisorbed anion. The mechanisms presented in this paper seem to be useful for explaining the epoxidation and complete oxidation of other olefins. A comparison with the previous studies is also presented.

Keywords: Ab initio Hartree–Fock (HF) and second-order Møller–Plesset (MP2) methods; Atomic oxygen; Catalytic activity of silver; Dipped adcluster model (DAM); Epoxidation vs. complete oxidation; Olefins; Propylene; Superoxide

1. Introduction

The epoxidation of olefins on silver catalyst is an exceedingly important catalytic reaction in industry, and as such has received long and extensive study (for reviews, see Refs. [1–7]). During the past 20 years, much research [1–32] has been devoted to gain a better understanding of the epoxidation mechanism with the ultimate goal of increasing the selectivity for the epoxide formation.

One particularly interesting aspect of the epoxidation reaction is its uniqueness: not only is silver a uniquely effective catalyst for heterogeneous epoxidation with molecular oxygen as oxidant, but also, ethylene is the only hydrocarbon that may be epoxidized with a high selectivity [1–7]. Recent experimental studies show that, except for ethy-

* Corresponding author. Fax: (+81) 75 7535910.

[1] Present address: Department of Chemistry, School of Science and Engineering, Waseda University, Ohkubo 3-4-1, Shinjuku-ku, Tokyo 169, Japan.

0039-6028/98/$19.00
PII: S0039-6028(98)00025-9

lene, a few olefins such as styrene [33,34], 3,3-dimethylbutene [35], norbornene [36] and butadiene can be epoxidized over silver with high selectivity. In contrast, other olefins such as propylene, butenes, and pentenes are epoxidized on silver with extremely low selectivity [8–14]. The selectivity reported for the formation of propylene oxide from propylene on silver is from 2 to 4% [8–11]. Due to this low selectivity, the industrial value of this reaction for the production of propylene oxide is quite limited, and considerably less attention has been paid to the oxidation of propylene on silver than to that of ethylene.

Previous studies have suggested that the lower epoxidation selectivity for propylene vs. ethylene is due both to a decreased rate of epoxidation of propylene [8] and to an increased rate of propylene combustion [8,12]. The increased favorability for propylene combustion has been attributed [8,14,27,28] to a greater reactivity of the allylic hydrogens in propylene compared to that of the vinyl hydrogens in ethylene. This was consistent with the observation of the isotope effect in the epoxidation of propylene: the selectivity increases by as much as 14% when the allylic hydrogen is replaced with deuterium [8,9].

For the oxidation of ethylene and propylene, two mechanisms involving molecular oxygen [8–18] and atomic oxygen [22–31] as the active species have been suggested. The mechanistic sketch summarized by Ayame [2–4] leads to a good insight into the mechanism of the epoxidation of ethylene. Based on the mechanism involving molecular oxygen, Cant and Hall [8] proposed that the dominant epoxidation mechanisms were similar for both ethylene and propylene, and the adsorbed species containing peroxide linkage was the common intermediate. The very low yield of epoxide from propylene was supposed to be due to the intramolecular isomerization of the peroxide intermediate to allylhydroperoxide by breaking the C–H bond of the methyl group. Akimoto et al. [14] proposed that the complete oxidation of propylene was initiated by the abstraction of allylic hydrogen of the adsorbed propylene by the adsorbed molecular oxygen.

Carter and Goddard [29] have used the generalized valence bond (GVB) method to calculate the energetics of the elementary steps for the olefin oxidation on the silver surface, and suggested that the surface atomic oxyradical anion (SAO) is the active species for the formation of ethylene oxide. The possible reaction mechanism for the combustion of higher olefins such as propylene, competing effectively with the epoxidation, was supposed to be due to the formation of alkoxide intermediate. Recently, in contrast to the result of Carter and Goddard, Madix et al. [27,28] showed that the combustion of propylene via an allylic intermediate was facile on Ag(110) with the oxygen coverages from 0.05 to 0.5 ML, and proposed that the dominant mechanism for the combustion of propylene and higher alkenes over silver is the activation of the allylic C–H bond via an acid–base reaction.

Theoretical studies on the epoxidation reactions of olefins are quite limited. Though a few papers [29–32] have been published for the epoxidation of ethylene, almost no discussions were presented [29,32] for the oxidation of propylene, and the calculations did not explicitly include the surface contribution. The main difficulty in the theoretical studies was how to describe chemisorption species and calculate adsorption energy correctly using only small clusters. This may be the reason why no ab initio theoretical study for the full reaction pathway and the associated energy diagrams of the epoxidation reaction of olefins has been reported.

In a series of our previous studies [37–46], a theoretical model named dipped adcluster model (DAM) [37,38] has been proposed to study chemisorptions and surface reactions involving electron transfer between admolecules and surfaces. The DAM has been successfully applied to the harpooning, surface chemiluminescence and electron emission in the halogen/alkali-metal surface system [42], and to the study of the oxygen chemisorption species on a silver surface [39–41]. Most recently, we used this model to study the mechanisms of the reaction of ethylene both with molecularly and atomically adsorbed oxygen on a silver surface [43], and for the first time, we could obtain the total reaction pathway and energy diagrams for the epoxidation reaction of ethylene on a silver surface. The uniqueness of the silver surface for ethylene epoxidation reaction has been clarified by

a comparative study of the stability and the activity of oxygen species on Cu, Ag, and Au surfaces [44]. The nature of the transition state (TS) in the reaction of the atomically adsorbed oxygen with ethylene to ethylene oxide has been studied in detail [47], since it is the key step to increase the overall selectivity in the epoxidation of ethylene on a Ag surface. The electron back-transfer from the adcluster to the bulk Ag surface at this TS has been clarified [47]. Thus, the DAM was essential for the study of these surface reactions. Even a small DAM could be used to give correct electronic structures and reliable adsorption energies in contrast to the cluster model [45].

In this paper, we investigate the mechanisms for the epoxidation and complete oxidation of propylene on a silver surface using the DAM combined with the ab initio Hatree–Fock (HF) and second-order Møller–Plesset (MP2) calculations. The aim is to address why some higher olefins mainly undergo complete oxidation instead of epoxidation. Several postulated pathways for both the epoxidation and complete oxidation are investigated, and both molecularly and atomically adsorbed oxygen species are examined. The paper is organized as follows. Section 2 gives the outline of the computational details. In Section 3, we study the mechanism similar to that of ethylene reported in the former paper [43]. In Section 4, the mechanistic details for the activation of allylic C–H bond are reported. An overall discussion based on the present results compared with the previous studies is given in Section 5, and finally in Section 6, we give the conclusion of the present study.

2. Computational details

We use the DAM [37,38] that has been proposed as a theoretical model for studying chemisorptions and surface reactions involving electron transfer between bulk metal and admolecules with consideration of the image force correction. Such interactions were found to be very important in the previous studies [37–46] for studying the chemisorptions and the reactions of the oxygen on a metal surface.

As active oxygen species, we study molecularly adsorbed superoxide in an end-on bent structure (Fig. 1a) and the atomically adsorbed oxygen (Fig. 1b). The validity of the similar model has been shown in the study of the mechanism of ethylene epoxidation on Ag [43], Cu, and Au [44]. The electron exchange between the adcluster and the bulk metal is taken into account by the DAM. Since we use the highest spin coupling model [37,38], the number of electrons transferred into the adcluster is unity ($n=1$) as shown previously [39–41]. The electrostatic interaction between the admolecule and the extended surface is estimated by the image force correction [38]. We calculate the potential energy of the adcluster by the ab initio HF and MP2 methods. The geometries of the reactants, products, intermediates, and transition states (TSs) are optimized by the energy gradient method at the HF level except for the Ag–Ag distance and the Ag_2–Ag_1–O_a angle that were fixed at 2.8894 Å and 90.0°, respectively. The electron correlations are considered by the MP2 method. The energy scale is, in all cases, in kilocalories per mole (kcal mol^{-1}), and the bond distance scale is in angstroms (Å). The calculations are

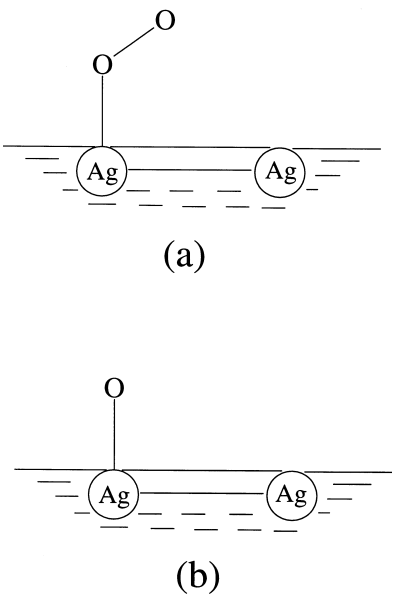

Fig. 1. Adsorption structure of oxygen on silver surface. (a) Molecularly adsorbed oxygen in end-on bent geometry. (b) On-top form of atomically adsorbed oxygen.

performed using the Gaussian 92 software package [48].

The Gaussian basis for the silver atom is (3s3p4d)/[3s2p2d] set, and the Kr core was replaced by the relativistic effective core potential [49]. For oxygen, we used the (9s5p)/[4s2p] set of Huzinaga–Dunning [50,51] augmented by the diffuse s and p functions of $\alpha=0.059$ as anion bases [52]. The polarization d functions of $\alpha=$ 2.704, 0.535 [53] were added to the oxygen basis in the MP2 calculations. For carbon and hydrogen, the (9s5p)/[4s2p] and (4s)/[2s] sets, respectively, of Huzinaga–Dunning were used [50,51]. The validity of the present basis functions as well as the effects of electron correction have been carefully examined in the former paper [43]. The heats of reactions for the epoxidation and complete oxidation of propylene were calculated to be 23.9 and 456.6 kcal mol^{-1}, respectively, in the MP2 calculation using the present basis set, which compare well with the experimental values, 27.5 and 460.3 kcal mol^{-1}, respectively.

3. Mechanisms via the C=C double bond breakage

A common view of the epoxidation mechanism assumed that the reaction takes place between the adsorbed oxygen species and the carbon of the C=C double bond of olefins. Our previous study has shown that this was certainly true for the epoxidation of ethylene [43]. Some studies [8–11,29,32] had assumed that the epoxidation mechanism for ethylene and propylene may be similar. We begin in this section with the investigation of the mechanisms for the epoxidation and complete oxidation of propylene via the C=C double bond breakage and compare the result with those of ethylene.

3.1. Reaction with superoxide O_2^- on silver

A difference between propylene and ethylene is that propylene has two different olefinic carbons. Therefore, in double bond opening, two radical intermediates, i.e. $CH_3CH\cdot$–CH_2–O–O–Ag and $\cdot CH_2$–$CH(CH_3)$–O–O–Ag should be considered. Then, we study here the reactions of two different olefinic carbons with the molecularly adsorbed superoxide species on a silver surface. The most favorable pathway for the attack on the C=C double bond takes the form of Figs. 2a or b.

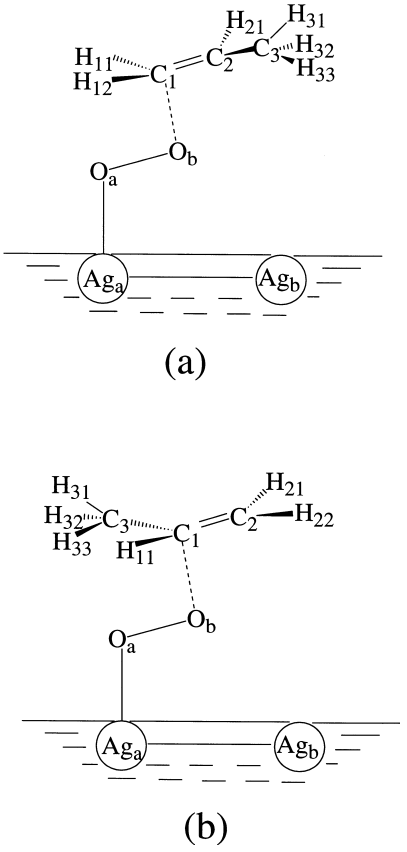

Fig. 2. Model adcluster for the olefinic carbon attack (a) on the terminal olefinic carbon, and (b) on the central olefinic carbon.

Fig. 3 shows the energy diagrams for the oxidation reactions between molecular superoxide and propylene at the terminal carbon atom (Fig. 2a). The diagram leading to propylene oxide (PRO) is denoted by a solid line, and that to aldehyde and then to complete combustion is denoted by the dashed line. The optimized structures of the intermediates and the TSs are also illustrated.

An obvious point deduced from Fig. 3 is that the energy diagram for the oxidation of propylene is very similar to that of ethylene reported in the previous paper [43]. It certainly reflects some common features between the reactions of the two

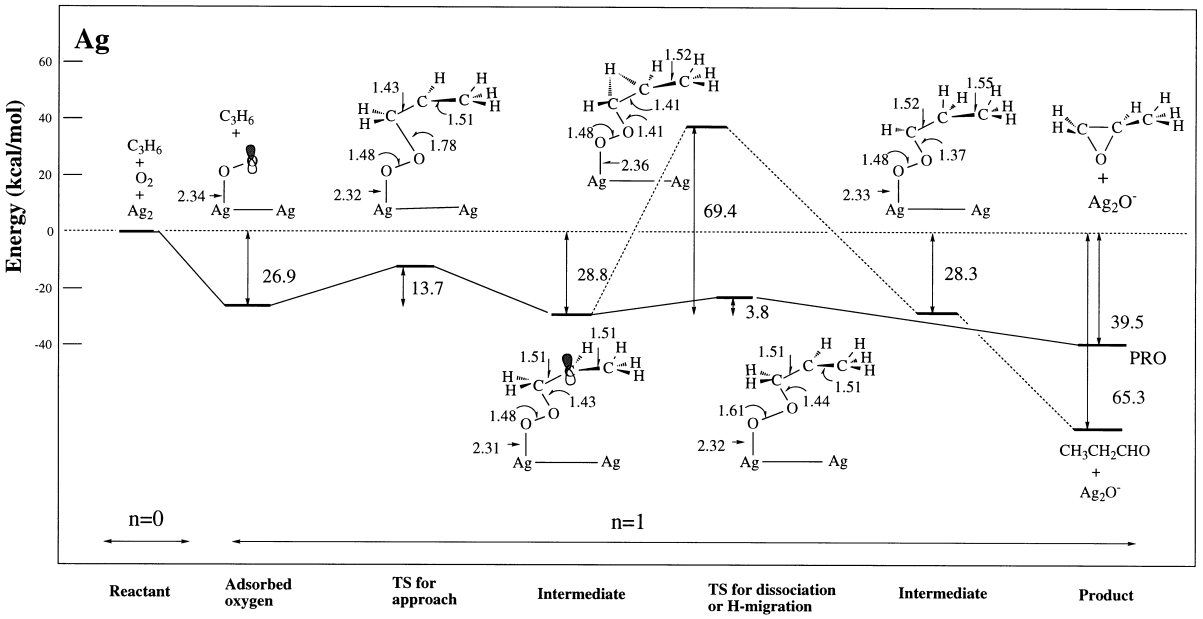

Fig. 3. Energy diagram for the reaction between terminal carbon atom of propylene and molecularly adsorbed superoxide on Ag surface. The routes leading to propylene oxide and aldehyde are shown by the solid and broken lines, respectively.

olefins when it takes place via the C=C double bond breakage.

The reaction proceeds by the two-step mechanism. The first step is the formation of the superoxide species on the Ag surface in which one electron is transferred from the bulk metal to the adcluster. The calculated stabilization for this step is 26.9 kcal mol^{-1}, which is the same as in the previous paper [43]. The next step is the attack of the olefin on to the terminal oxygen atom O_b, the reactive site of the superoxide, in the geometry shown in Fig. 2a. The process reaching the TS includes the formation of a σ bond between O_b and C_1 and the breaking of the C–C π bond, and the energy barrier for this step is 13.7 kcal mol^{-1} at R_{co} of 1.78 Å. The system then arrives at the intermediate shown in Fig. 3 with the calculated stabilization energy of 28.8 kcal mol^{-1}. In this state, one carbon atom C_1 of propylene is bound to the terminal oxygen O_b of the molecularly adsorbed oxygen, and the π bond between C_1 and C_2 is broken with C_2 being the radical center. The C–C bond of this intermediate rotates almost without any barrier, giving a mixture of the geometrical isomer as shown previously for the reaction of ethylene [43]. In fact, both *cis*-/*trans*-PRO-D_2 and *cis*-/*trans*-PRO-D_5 molecules were produced from the oxidation of *cis*-CH_3CDCHD and *cis*-CD_3CDCHD, respectively [9].

When this intermediate is produced, the formation of propylene oxide is a fast process, leaving the atomic oxygen on the Ag surface: the energy barrier of this process is only 3.8 kcal mol^{-1}. The heat of reaction is calculated to be 39.5 kcal mol^{-1}, which represents the heat of reaction of gaseous propylene oxide plus half of the dissociative adsorption energy of O_2 on Ag_2, i.e. 23.9 and 15.6 kcal mol^{-1}, respectively, by the MP2 method.

In contrast, the process leading to propylene aldehyde from this intermediate must overcome a large energy barrier as high as 69.4 kcal mol^{-1}. In Fig. 3, this process is shown by a broken line. The energy diagram up to this intermediate is common to the above case. The high barrier is caused by a difficulty of α-H migration, though afterwards, the process is energetically favorable giving aldehyde,

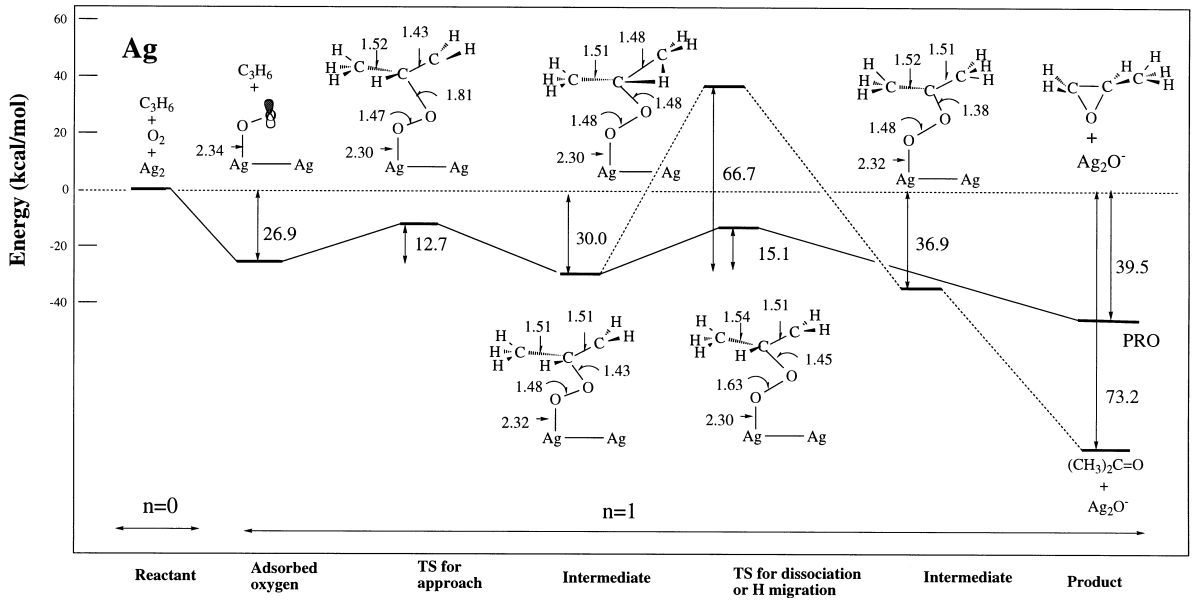

Fig. 4. Energy diagram for the reaction between central carbon atom of propylene and molecularly adsorbed superoxide on Ag surface. The route leading to propylene oxide and aldehyde are shown by the solid and broken lines, respectively.

which is considered to be further oxidized to CO_2 and H_2O. Thus, the path leading to complete oxidation is energetically forbidden.

The result given in Fig. 3 thus implies that the epoxidation of propylene should occur in high selectivity as for ethylene, but this is in contradiction with the experimental fact. Why? We want to answer this question in Section 4, but before that, let us examine another reaction path defined by Fig. 2b.

The energy diagram for the reaction involving the attack of the superoxide on the central carbon of propylene as shown in Fig. 2b is shown in Fig. 4. Comparing Fig. 4 with Fig. 3, we see that the two energy diagrams are essentially the same except for some rather small differences. First, the energy barrier leading to epoxide is 15.1 kcal mol^{-1}, which is 11.3 kcal mol^{-1} higher than that for the pathway shown in Fig. 3. The energy barrier for the α-H migration is, however, almost the same as in Fig. 3, but the stability of the products increases by about 9 kcal mol^{-1}. Though the two paths give the same epoxidation product, the aldehyde products are different. The first route gives propylene aldehyde, while the second gives acetone. Besides these differences, the second reaction given in Fig. 4 also shows a highly selective production of propylene oxide in contrast to the experimental fact.

The optimized geometries in these pathways are shown in Figs. 3 and 4. Table 1 shows the normal mode having the negative force constant at the TS. We refer to such a normal mode as an imaginary mode. The changes in the O_a–O_b, O_b–C_1 and C_1–C_2 distances, and the mode of the negative force constant at TS, clearly reflect the progress of the reaction along the path. Tables 2 and 3 show the net charge and the frontier density (spin population) of the $Ag_2O_2C_3H_6$ adcluster, calculated by the MP2 method as the reaction proceeds as shown in Figs. 3 and 4, respectively. In comparison with the change in the net charge, the frontier density changes significantly as the reaction proceeds: the reactive site shifts with the spin moving from one atom to another. From Table 2, we see that in the adsorbed superoxide, the reactive site is O_b with a frontier density of +0.784, while in the intermediate state, the C_2 atom becomes most

Table 1
Normal modes having the negative force constants at the TSs shown in Figs. 3 and 4[a]

TS structure	Eigen value	Term	Eigen vector
TS1 for approach	−0.092	C_1–O_b stretching	0.973
		C_1–C_2 stretching	−0.168
TS1 for dissociation	−0.170	O_a–O_b stretching	−0.964
		O_a–O_b–C_1 bending	0.140
TS2 for approach	−0.169	C_1–O_b stretching	0.950
		C_1–C_2 stretching	−0.166
TS2 for dissociation	−0.145	O_a–O_b stretching	−0.980
		O_a–O_b–C_1 bending	0.118

[a]The TSs shown in Fig. 3 are denoted as TS1, and those shown in Fig. 4 are denoted as TS2, respectively.

Table 2
Net charge and frontier density (spin population) for the Ag_2O_2–C_3H_6 adcluster shown in Fig. 3

	Adsorbed oxygen	TS for appro.	Intermediate	TS for dissoc.	TS for H mig.	IM for CH_3CH_2CHO
Net charge						
Ag_1	−0.028	−0.058	−0.033	−0.035	−0.014	−0.021
Ag_2	−0.197	−0.275	−0.307	−0.316	−0.273	−0.276
O_a	−0.558	−0.616	−0.641	−0.658	−0.714	−0.635
O_b	−0.217	−0.319	−0.290	−0.273	−0.213	−0.261
C_1	−0.496	−0.085	0.003	−0.005	0.088	0.113
C_2	−0.021	−0.119	−0.147	−0.147	−0.343	−0.397
C_3	−0.580	−0.641	−0.635	−0.634	−0.602	−0.621
H_{11}	0.182	0.186	0.152	0.162	0.184	0.162
H_{12}	0.191	0.191	0.158	0.166	0.170	0.163
H_{21}	0.180	0.161	0.160	0.159	0.180	0.170
H_{31}	0.175	0.227	0.236	0.223	0.209	0.265
H_{32}	0.183	0.184	0.179	0.186	0.165	0.169
H_{33}	0.183	0.164	0.165	0.165	0.209	0.169
Frontier density						
Ag_1	+0.182	−0.009	0.017	−0.036	−0.004	0.006
Ag_2	−0.169	0.021	0.022	0.051	0.002	−0.009
O_a	+0.203	0.475	−0.022	−0.291	0.052	0.065
O_b	+0.784	−0.183	0.055	0.323	0.063	0.044
C_1	0.0	−0.155	−0.107	−0.127	0.974	1.004
C_2	0.0	0.953	1.183	1.191	−0.089	−0.118
C_3	0.0	−0.107	−0.133	−0.135	0.042	0.005
H_{11}	0.0	0.003	0.006	0.011	−0.015	−0.068
H_{12}	0.0	0.001	0.006	0.006	−0.082	0.032
H_{21}	0.0	−0.072	−0.085	−0.087	0.056	0.040
H_{31}	0.0	0.007	0.019	0.015	−0.004	−0.001
H_{32}	0.0	0.048	0.063	0.063	0.007	−0.001
H_{33}	0.0	0.018	0.010	0.016	−0.002	0.000

reactive with a spin population of 1.183. A similar behavior is also seen from Table 3. The energy barrier is actually the barrier for the spin transfer.

We note that the net charges of the Ag atoms are relatively small (less than $\sim$0.3) throughout the reaction, and the frontier density on silver is almost zero in the course of the reaction. This means that the additional electron transferred from

Table 3
Net charge and frontier density for the Ag_2O_2–C_3H_6 adcluster shown in Fig. 4

	Adsorbed oxygen	TS for appro.	Intermediate	TS for dissoc.	TS forH mig.	IM. for$CH_3C(O)CH_3$
Net charge						
Ag_1	−0.028	−0.082	−0.058	−0.120	−0.050	−0.053
Ag_2	−0.197	−0.315	−0.307	−0.305	−0.260	−0.290
O_a	−0.558	−0.594	−0.629	−0.350	−0.709	−0.664
O_b	−0.217	−0.263	−0.269	−0.481	−0.301	−0.235
C_1	−0.496	0.273	0.302	0.373	0.472	0.496
C_2	−0.021	−0.493	−0.448	−0.485	−0.816	−0.724
C_3	−0.580	−0.687	−0.672	−0.699	−0.716	−0.699
H_{11}	0.182	0.178	0.144	0.141	0.436	0.220
H_{21}	0.191	0.182	0.169	0.172	0.185	0.187
H_{22}	0.180	0.179	0.175	0.171	0.152	0.177
H_{31}	0.175	0.287	0.257	0.256	0.246	0.238
H_{32}	0.183	0.156	0.156	0.154	0.171	0.148
H_{33}	0.183	0.181	0.181	0.178	0.171	0.200
Frontier density						
Ag_1	+0.182	−0.011	−0.020	−0.015	−0.008	−0.013
Ag_2	−0.169	0.045	0.034	0.029	0.017	0.014
O_a	+0.203	0.490	−0.072	0.304	0.067	−0.007
O_b	+0.784	−0.198	0.101	−0.301	−0.021	0.133
C_1	0.0	−0.160	−0.117	−0.062	0.978	0.937
C_2	0.0	0.973	1.232	1.209	−0.090	−0.109
C_3	0.0	−0.004	0.003	−0.002	−0.093	−0.094
H_{11}	0.0	0.000	0.006	−0.001	0.034	0.010
H_{21}	0.0	−0.066	−0.084	−0.083	0.032	0.060
H_{22}	0.0	−0.066	−0.084	−0.081	0.023	0.007
H_{31}	0.0	−0.001	−0.001	−0.000	0.023	0.008
H_{32}	0.0	−0.004	0.002	0.005	0.009	0.030
H_{33}	0.0	0.001	0.000	−0.003	0.030	0.024

the bulk metal to the adcluster in the DAM lies mainly on the admolecule throughout the course of the reaction.

3.2. Reactions with atomically adsorbed oxygen

We investigate in this section the energetics and the pathway of the reaction of the olefinic carbon with the atomically adsorbed oxygen on an Ag surface. The net charge and the frontier density of the atomically adsorbed oxygen on the silver surface are calculated to be −0.642 and +1.031, respectively. The charge is largely negative, more negative than the O_a (inside) atom of the superoxide shown in Table 2. The spin exists on the in-plane 2p orbital, which is parallel to the Ag–Ag bond. Therefore, the most favorable approach of propylene to form the C_1–O bond takes place in the form illustrated in Fig. 5.

Fig. 5 shows the geometries and the energy diagram in the course of the reaction. Table 4 shows the net charge and the spin population of each atom. In the TS approach, the C_1–O bond is formed by the interaction between the in-plane p orbital of O and the π and π^* orbitals of propylene. The C_1–O distances in the TS and the intermediate are calculated to be 1.86 and 1.42 Å, respectively. The C–C bond distance changes from 1.35 Å in the reactant to 1.42 Å in the TS, and further to 1.52 Å in the intermediate: it changes from the double-bond length to the single-bond one. The calculated stabilization energy of the intermediate is 35.1 kcal mol^{-1}. The energy barrier to this intermediate is calculated to be −1.0 kcal mol^{-1}, which

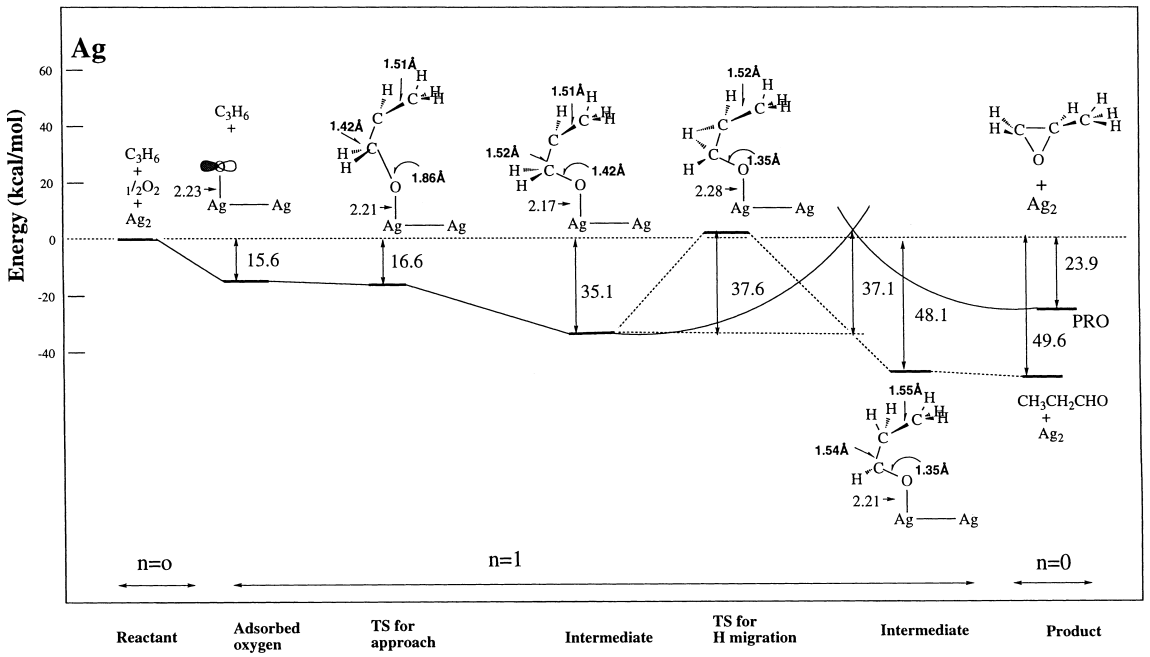

Fig. 5. Energy diagram for the reaction between terminal carbon atom of propylene and atomically adsorbed oxygen on Ag surface. The routes leading to propylene oxide and aldehyde are shown by the solid and broken lines, respectively.

means that no or little barriers exist in this path and reflects the high reactivity of the atomically adsorbed oxygen. The negative energy barrier here is due to the present somewhat inconsistent calculations: the geometry was optimized by the HF method, and the energy was calculated by the MP2 method. In the HF level, this energy barrier was 27.4 kcal mol^{-1}, a positive value.

The next step from this intermediate was very important for the ethylene oxidation in the former paper [43], since it determines the selectivity of the reaction by the atomically adsorbed oxygen. If C_2 attacks the oxygen to form the C_2–O_b bond, propylene epoxide is formed. If C_2 attacks the α-C–H bond, causing the hydrogen migration as shown in Fig. 5, the aldehyde is a product that is further oxidized to CO_2 and H_2O, the complete oxidization product.

For the hydrogen migration reaction, the barrier was calculated to be 37.6 kcal mol^{-1}, which is lower than the barrier 69.4 kcal mol^{-1} of the reaction in which the superoxide species is involved (see Fig. 3). This means that the complete oxidation has a greater chance of taking place by the reaction with atomically adsorbed oxygen. The structure of the TS to the epoxide formation was, however, difficult to determine, and the corresponding energy barrier could not be presented. However, if we take the crossing point of the $n=1$ and $n=0$ curves as the barrier of this process, the energy barrier is almost the same as that for the complete oxidation path, showing a competition of the two reaction path. This shows that the atomically adsorbed oxygen is not selective for the epoxidation of propylene, as it was so for the epoxidation of ethylene [43].

4. Mechanism via allylic C–H bond activation

The results presented above show that the reaction between propylene and adsorbed oxygen via the C=C double bond breakage is favorable for the epoxide formation likewise in the reaction of ethylene. However, experimentally, the oxidation of ethylene and propylene over the same catalysts produces markedly different products: propylene is mainly oxidized to CO_2 and H_2O. The observed

Table 4
Net charge and frontier density for the $Ag_2O–C_3H_6$ adcluster shown in Fig. 5

	Adsorbed oxygen	TS for approach	Intermediate	TS for H migration	Intermediate for CH_3CH_2CHO
Net charge					
Ag_a	−0.058	−0.195	−0.219	−0.150	−0.167
A_b	0.300	−0.248	−0.272	−0.252	−0.269
O_a	−0.642	−0.651	−0.651	−0.638	−0.599
C_1	−0.496	−0.180	−0.029	−0.010	0.066
C_2	−0.021	−0.117	−0.140	−0.296	−0.380
C_3	−0.580	−0.655	−0.636	−0.642	−0.630
H_{11}	0.182	0.150	0.107	0.154	0.094
H_{12}	0.191	0.158	0.136	0.126	0.154
H_{21}	0.180	0.156	0.165	0.205	0.145
H_{31}	0.175	0.163	0.165	0.162	0.284
H_{32}	0.183	0.255	0.253	0.169	0.152
H_{33}	0.183	0.164	0.154	0.173	0.151
Frontier density					
Ag_a	−0.108	0.356	0.036	−0.008	−0.017
Ag_b	0.077	−0.331	−0.015	0.009	0.015
O_a	1.031	0.460	0.022	0.105	0.165
C_1	0.0	−0.317	−0.085	0.442	0.938
C_2	0.0	0.902	1.155	0.545	−0.108
C_3	0.0	−0.096	−0.128	−0.041	0.006
H_{11}	0.0	0.015	0.008	−0.054	−0.061
H_{12}	0.0	0.011	0.000	−0.002	0.034
H_{21}	0.0	−0.066	−0.082	−0.031	0.031
H_{31}	0.0	0.030	0.027	0.001	−0.001
H_{32}	0.0	0.034	0.059	0.004	−0.001
H_{33}	0.0	0.001	0.004	0.028	−0.001

much lower selectivity, i.e. 2–5%, of propylene to epoxide than that of ethylene is therefore not understandable based on the reaction mechanism discussed above.

In this section, we investigate a different oxidation pathway of propylene via an allylic hydrogen activation. The reaction pathway first posturated and finally concluded in this section is illustrated in Fig. 6. The reaction with the molecularly adsorbed superoxide species is given in the upper part, and that with the atomically adsorbed oxygen is given in the lower part. Though the detailed explanation is given below, the point is the formation of the (O)–O–H species and the allylic anion adsorbed on a Ag surface. The symmetry of the reaction is C_1: the allylic CCH and (O)–O–Ag_2 are in the same plane, and the other part of propylene is out of plane.

4.1. Reaction with molecularly adsorbed oxygen

We use the model adcluster illustrated in Fig. 7a to study the reaction of the allylic hydrogen of propylene with the molecularly adsorbed superoxide. A two-step path is involved there as illustrated in Fig. 6a: the allylic hydrogen abstraction step and the O–O decomposition step. In the first step, the allylic hydrogen of propylene is abstracted by the terminal oxygen of the superoxide, leading to the adsorbed hydroperoxyl species [$HOO_{(a)}$] and the adsorbed allyl species [$C_3H_{5(a)}$]. The next step is the decomposition of the adsorbed hydroperoxyl group to the adsorbed surface hydroxyl group [$HO_{(a)}$] and the adsorbed atomic oxygen [$O_{(a)}$]. Two surface hydroxyl groups can be disproportionated to produce water and one adsorbed oxygen [28,29]. The adsorbed oxygen atom pro-

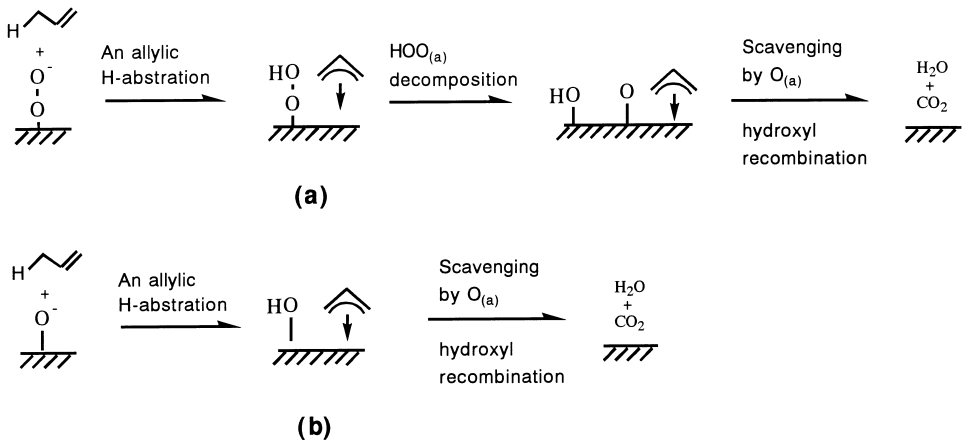

Fig. 6. Mechanism of the complete oxidation of propylene over silver surface. (a) Reaction with molecularly adsorbed superoxide. (b) Reaction with atomically adsorbed oxygen.

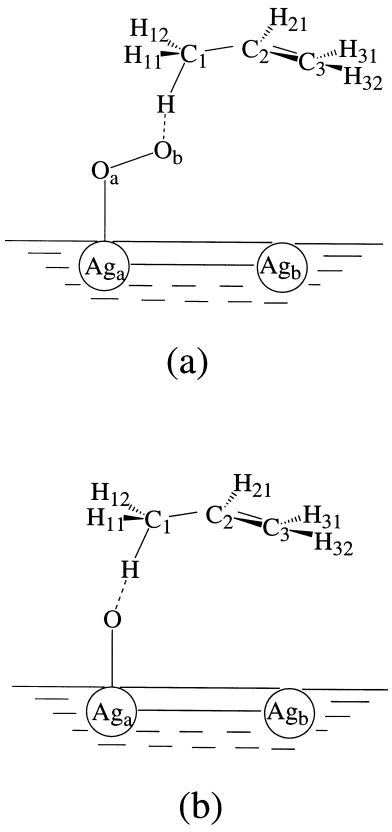

Fig. 7. Model adcluster for the allylic H attack mechanism. (a) Reaction with molecularly adsorbed superoxide. (b) Reaction with atomically adsorbed oxygen.

duced in this process has the reactivity to process a further oxidation reaction, which will be studied below in this section. The adsorbed hydrocarbon species should be readily oxidized to CO_2 and H_2O in the presence of adsorbed oxygens, though the detailed mechanism of the further oxidation is not clear.

Fig. 8 shows the fully optimized geometries and the energy diagram for the first reaction step. The process reaching to the TS includes the formation of a σ bond between an allylic hydrogen and the terminal oxygen atom (O_b) and the breakage of the σ bond between this hydrogen and C_1 atom. The H_a–O_b distance is 1.17 Å, and the C_1–H_a distance is 1.38 Å which is elongated by about 0.3 Å in comparison with 1.09 Å in the free propylene molecule. The O_a–O_b distance is also elongated from 1.39 Å in the adsorbed superoxide state to 1.47 Å. The C_1–C_2 and C_2–C_3 distances are also different to the typical C–C single and C=C double bonds, respectively, but the charges are small. The imaginary mode at TS shown in Table 5 clearly shows the nature of the TS in this reaction path, i.e. O_b–H and C_1–H stretching.

The energy barrier in this first step is calculated to be 10.8 kcal mol^{-1}, which is smaller than those of 13.7 and 12.7 kcal mol^{-1} for the reactions leading to the epoxide shown in the preceding section. This shows that the pathway via the abstraction of the allylic hydrogen is easier. The stabilization

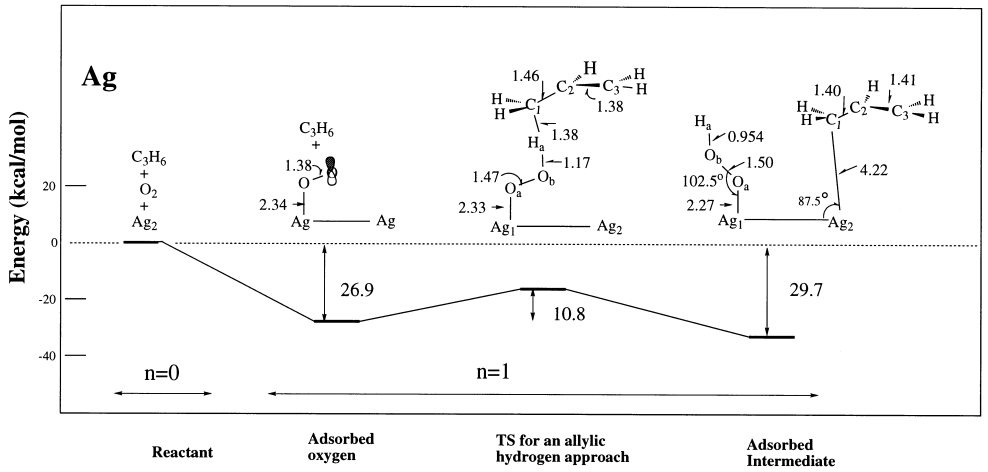

Fig. 8. Energy diagram for the reaction between molecularly adsorbed oxygen and allylic hydrogen of propylene on silver surface.

Table 5
Normal modes having the negative force constants at the TSs shown in Figs. 8 and 9

TS structure	Eigen value	Term	Eigen vector
TS for approach	−0.232	O_b–H stretching	−0.682
		H–C_1 stretching	0.639
		H_{11}–C_1–C_2 bending	0.151
		$H_{11}C_1C_2O_b$ torsion	−0.257
TS for O–O dissociation	−0.140	O_a–O_b stretching	−0.928
		H–O_a–O_b bending	0.369

energy after the barrier at the intermediate is 29.7 kcal mol^{-1} as shown in Fig. 8 in comparison with 28.8 and 30.0 kcal mol^{-1} for the stabilization energy of the intermediates shown in Figs. 3 and 4. The geometry of this intermediate state given in Fig. 8 shows that the allyl group is adsorbed to the surface very weakly, due to the small cluster used here. We note that the allyl group would be more stably adsorbed on the surface as discussed later, and the actual stabilization energy in the adsorbed intermediate state would be larger than the energy obtained here.

Fig. 9 shows the calculated results for the second reaction step: the decomposition of the adsorbed hydroperoxyl group. The geometry optimization was carried out assuming the O–Ag–Ag angle to be rectangular. The hydroperoxyl group in the adsorbed intermediate shown in Fig. 8 is not stable because of the interaction with the allyl anion species adsorbed on the adjacent silver atom. The optimized geometry shown in Fig. 9, in which no such interaction exists, is very different to that in the final adsorbed intermediate shown in Fig. 8. In Fig. 9, the O_a–O_b distance and the O_bO_aAg angle are 1.532 Å and 84.9°, respectively, in comparison with 1.50 Å and 102.5° in Fig. 8. This change is caused by the interaction between O_b and the adjacent silver atom Ag_2. At the TS for dissociation, the O–O distance increases and the O–Ag_1 distance decreases, and the energy barrier is only 2.8 kcal mol^{-1}. After the TS, the system gains a very high stabilization energy of 42.6 kcal mol^{-1} and becomes the intermediate composed of the adsorbed hydroxyl group and the adsorbed oxygen atom. The net charge and frontier density shown in Table 6 reflect a shift of the reactive site from silver atom Ag_2 to O_a. The net charge and the frontier density of the adsorbed oxygen atom are −0.662 and +1.089, similar to −0.642 and +1.031 (see Table 4) of the free

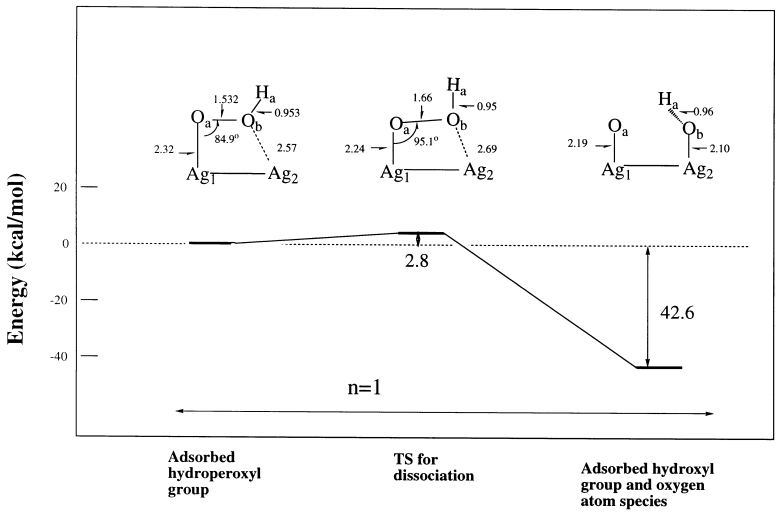

Fig. 9. Energy diagram for the decomposition of hydroperoxyl group on silver surface.

atomically adsorbed oxygen species. This atomically adsorbed oxygen should be active.

The mechanism that the complete oxidation of olefin proceeds via allylic hydrogen abstraction by molecular superoxide is supported by some experimental results. Tezuka et al. [54] showed in the oxidation of 9,10-dihydroanthracene that the superoxide ion is a hydrogen abstracting agent, and the initial step is the formation of radical intermediate and HO_2^- group. Moro-oka et al. [55] further studied the reactivity of the superoxide ion with some substrates having labile hydrogens, and indicated that the superoxide ion abstracts hydrogen from the substrate only when the formed radical can be stabilized by conjugating its π electrons. Hydrogen abstraction by the superoxide ion depends obviously on the C–H bond dissociation energy of the substrate, the borderline being roughly 80 kcal mol^{-1} at room temperature [55], which is similar to the C–H bond energy of propylene studied here.

4.2. Reaction with atomically adsorbed oxygen

The atomically adsorbed oxygen on the Ag surface is produced through the peroxide species of the molecularly adsorbed oxygen [42]. It is also produced, as shown in Fig. 9, as a product of the oxidation reaction of propylene with the molecularly adsorbed superoxide species. These two adsorbed atomic oxygen species have the same electronic structure and therefore, the same reactivity. We study in this section the reaction of the atomically adsorbed oxygen with propylene. A pictorial sketch of the reaction path is shown in Fig. 6b.

Fig. 10 shows the optimized reaction path and the energy diagram for the reaction of propylene with atomically adsorbed oxygen. Table 7 shows the net charge and frontier density for this reaction path. The geometry of the TS is similar to that of the reaction with the molecularly adsorbed oxygen shown in Fig. 8: it shows a formation of the σ bond between allylic hydrogen and oxygen atom and a breakage of the σ bond between this hydrogen and C_1 atom. The geometry of the adsorbed allyl group is also similar to that in Fig. 8, but the C_1–Ag_2 distance is shortened to 2.74 Å, which shows a stronger interaction between the allyl group and the surface. The reason of this change would be the neighboring effect of the adjacently hydroperoxyl adsorbed group, i.e. the steric and electrostatic effects of the hydroperoxyl group (HOO), as compared to hydroxyl one (HO), lead to a longer allyl carbon-surface distance. The calculated energy barrier in this reaction path is only $+0.1$ kcal mol^{-1}, which means that essentially no barrier exists in this reaction path. A

Table 6
Net charge and frontier density for the adcluster shown in Figs. 8 and 9

	Adsorbed oxygen	TS for H-appro.	Adsorbed intermediate	Adsorbed HOO species	TS for HO_2 dissoc.	Adsorbed O and HO species
Net charge						
Ag_1	−0.028	−0.073	0.012	−0.053	−0.107	0.092
Ag_2	−0.197	−0.224	−0.291	−0.210	−0.180	0.187
O_a	−0.558	−0.597	−0.611	−0.689	−0.645	−0.662
O_b	−0.217	−0.384	−0.574	−0.516	−0.541	−1.109
H_a	0.182	0.405	0.443	0.467	o.473	0.493
C_1	−0.580	−0.549	−0.323			
C_2	−0.021	0.009	−0.068			
C_3	−0.496	−0.523	−0.494			
H_{11}	0.183	0.205	0.196			
H_{12}	0.183	0.206	0.200			
H_{21}	0.175	0.168	0.163			
H_{31}	0.191	0.169	0.163			
H_{32}	0.180	0.187	0.184			
Frontier density						
Ag_1	+0.182	0.487	−0.013	0.876	0.903	0.457
Ag_2	−0.169	−0.512	0.022	1.155	1.118	0.388
O_a	+0.203	0.424	−0.012	−0.067	0.067	1.089
O_b	+0.784	−0.028	0.008	0.040	−0.093	0.070
H_a	0.0	0.000	0.000	−0.004	0.005	−0.003
C_1	0.0	0.560	0.829			
C_2	0.0	−0.185	−0.408			
C_3	0.0	0.349	0.780			
H_{11}	0.0	−0.028	−0.057			
H_{12}	0.0	−0.030	−0.058			
H_{21}	0.0	−0.001	0.017			
H_{31}	0.0	−0.018	−0.052			
H_{32}	0.0	−0.017	−0.053			

similar result was also presented in Section 3.2. The stabilization energy of the adsorbed intermediate is 38.3 kcal mol^{-1} as shown in Fig. 10, which is slightly more stable than the adsorbed intermediate shown in Section 3.2 (35.1 kcal mol^{-1} as shown in Fig. 5).

The formation of the adsorbed stable allyl group is a key factor for the reaction path discussed above. In order to understand the nature of the interaction between the allyl species and the silver surface more clearly, we further carried out a separate comparable calculation using $Ag_2C_3H_5$ adcluster.

Fig. 11 shows the results for the $Ag_2C_3H_5$ adclusters calculated with and without electron supply from the bulk metal, respectively. The net charge and frontier density are listed in Table 7. The geometries are very similar in the two adsorbed species, the C_1–Ag distances are 2.28 Å and 2.36 Å, and the calculated stabilization energy is 7.9 kcal mol^{-1} and 18.1 kcal mol^{-1} for the $n=0$ and $n=1$ calculations, respectively. The net charge of C_3H_5 is −0.27 and −0.52, respectively. These indicate that the allyl intermediate on the silver surface is anionic in nature. The evidence for the anionic nature had been reported experimentally by Madix et al. [27,28,56].

5. Overall discussion

Figs. 12 and 13 show the comparisons of the energy diagrams for the reaction via the C=C double bond breakage presented in Section 3 and

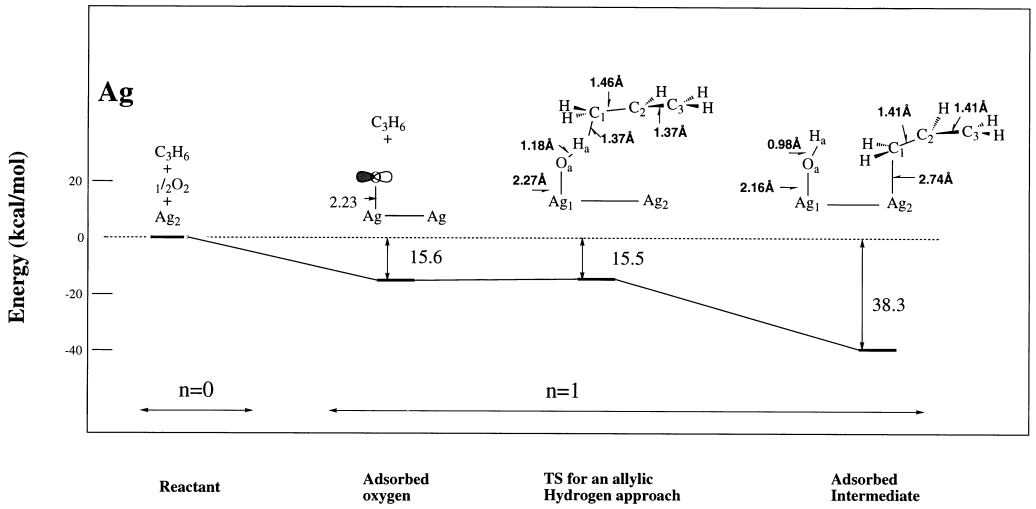

Fig. 10. Energy diagram for the reaction between allylic hydrogen of propylene and atomically adsorbed oxygen on silver surface.

Table 7
Net charge and frontier density for the adclusters shown in Figs. 10 and 11

	Adsorbed oxygen	TS for H-appro.	Adsorbed intermediate	Free Ag_2 and C_3H_5	Adsorbed radical species	Anionic adsorbate
Net charge						
Ag_a	−0.058	−0.051	0.038	0.000	0.176	−0.265
Ag_b	0.300	−0.279	−0.042	0.000	0.095	−0.212
O_a	−0.642	−0.949	−1.184			
H_a	0.175	0.395	0.440			
C_1	−0.580	−0.512	−0.566	−0.472	−0.718	−0.712
C_2	−0.021	0.023	0.019	0.016	0.059	0.087
C_3	−0.496	−0.523	−0.576	−0.472	−0.600	−0.661
H_{11}	0.183	0.185	0.218	0.188	0.205	0.156
H_{12}	0.183	0.185	0.231	0.184	0.197	0.149
H_{21}	0.175	0.173	0.146	0.184	0.175	0.140
H_{31}	0.191	0.174	0.149	0.188	0.205	0.153
H_{32}	0.180	0.180	0.163	0.184	0.204	0.166
Frontier density						
Ag_a	−0.108	0.033	0.019	0.000	0.219	0.811
Ag_b	0.077	−0.006	0.023	0.000	0.712	1.034
O_a	1.031	0.349	−0.027			
H_a	0.0	−0.048	0.008			
C_1	0.0	0.641	0.736	0.809	0.039	0.140
C_2	0.0	−0.134	−0.399	−0.412	−0.118	0.674
C_3	0.0	0.265	0.603	0.809	0.181	−0.719
H_{11}	0.0	−0.035	0.020	−0.057	−0.009	−0.004
H_{12}	0.0	−0.036	0.020	−0.053	−0.003	0.006
H_{21}	0.0	−0.006	−0.004	0.019	0.013	−0.072
H_{31}	0.0	−0.012	0.006	−0.057	−0.018	0.066
H_{32}	0.0	−0.010	0.006	−0.053	−0.016	0.065

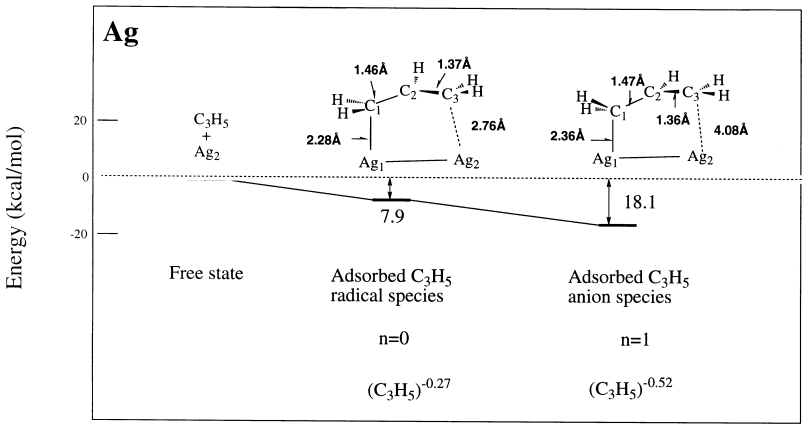

Fig. 11. Stability of the allyl species adsorbed on Ag_2 cluster in the neutral ($n=0$) and anion ($n=1$) adcluster states.

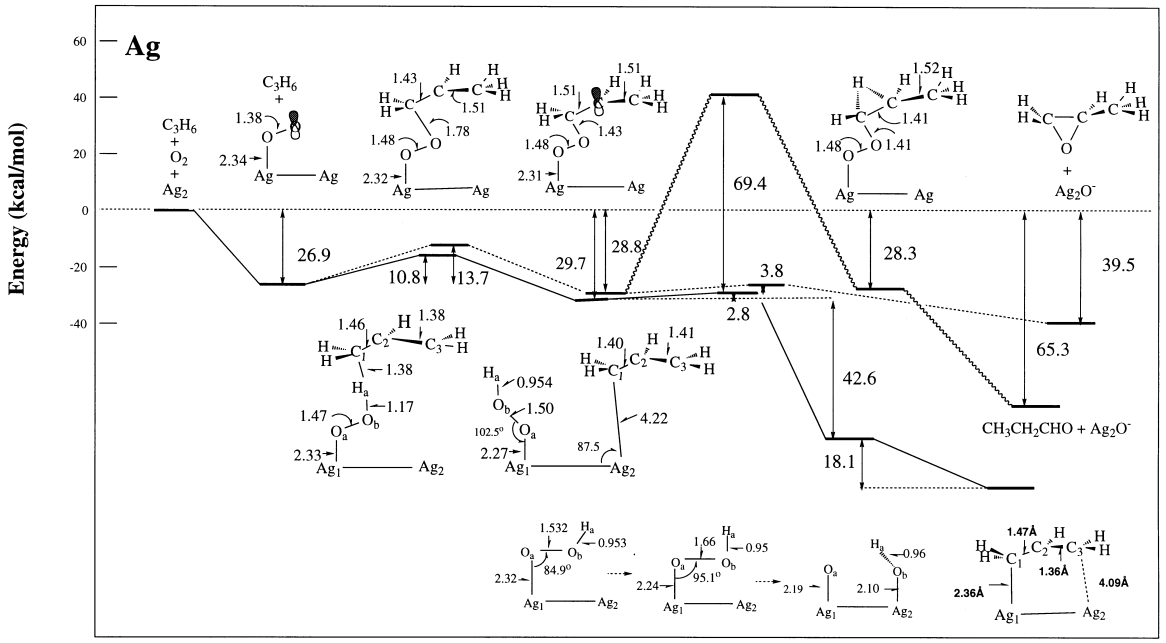

Fig. 12. Comparison of the energy diagram for the reactions between propylene and molecularly adsorbed oxygen. The route for allylic H attack is shown by the solid line, and those for carbon attack are shown by the broken and waved lines.

the reaction via allylic C–H breaking presented in Section 4. In both cases involving molecular and atomic oxygen species, the reaction path via allylic C–H breaking has lower energy barriers and more stable adsorbed intermediates. These results clearly show that the mechanisms via an allylic C–H breakage should have a greater chance of taking place with both molecularly adsorbed oxygen and atomically adsorbed oxygen. The low epoxide yield from propylene as compared with ethylene is mainly due to the activity of the allylic hydrogen and the stability of the allyl anion species on the Ag surface.

Based on the present results, we can reasonably explain the available experimental facts. The sharp contrast in the epoxide yield between propylene

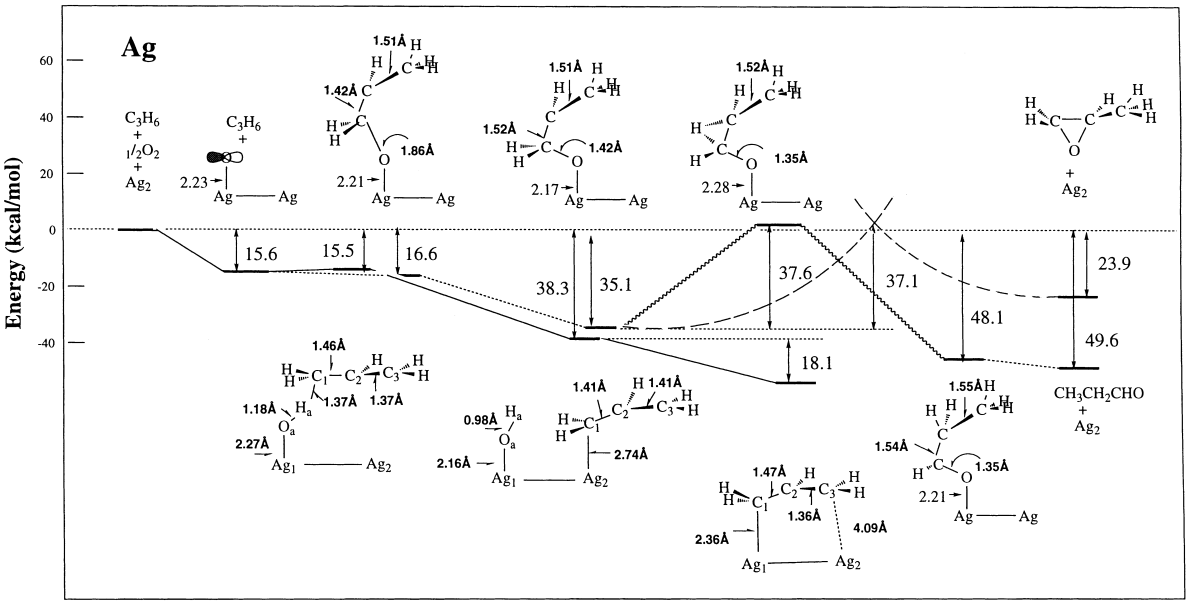

Fig. 13. Comparison of the energy diagram for the reactions between propylene and atomically adsorbed oxygen. The route for tallylic H attack is shown by the solid line, and those for carbon attack are shown by the broken and waved lines.

and ethylene is due to the existence and non-existence of the allylic hydrogen. The feasibility of the C–H bond breakage in propylene is due to the formation of the resonance-stabilized allyl radical or anion. Generally speaking, the olefins containing allylic C–H bonds, such as propylene, butenes and pentenes [14], suffer the complete oxidation initiated by the abstraction of the allylic hydrogen as shown in Section 4. Norbornene also possesses an allylic C–H bond, but no subsequent resonance-stabilized allyl radical or anion is formed, and therefore, it favors the epoxidation reaction initiated by the C=C double bond breakage as shown in Section 3. Ethylene, styrene, 3,3-dimethylbutene and butadiene contain no allylic C–H bonds, and therefore, they mainly produce the epoxides following the epoxidation mechanism as shown in Section 3.

The present theoretical results partially support some experimental findings. Early kinetic isotope effects with propylene for the oxidation of CD_3CHCH_2 and CD_3CDCD_2 studied by Cant and Hall [8] implied that further oxidation takes place by the reaction at the methyl group rather than at the vinyl or olefinic position. Akimoto et al. [14] studied the catalytic oxidation of ethylene, propylene, butenes, and pentenes over silver, and concluded that the complete oxidation of propylene is initiated by the abstraction of allylic hydrogen by the adsorbed molecular oxygen. Madix et al. [27,28] also proposed that the dominant mechanism for combustion of propylene and higher alkenes on silver is the activation of an allylic C–H bond. Further, π-allyl species have been demonstrated on a number of metal oxides active for propylene oxidation [57,58].

Cant and Hall [8] may have been the first to propose a mechanistic sketch for the oxidation of ethylene and propylene, and succeeded in explaining the observed kinetic isotope effects of the hydrogens for the formation of epoxide and CO_2. They assumed that the oxidation of olefins (ethylene and propylene) to epoxide and CO_2 takes place via the preliminary formation of an intermediate that is common to both product formations. The very low yield of epoxide from propylene is attributed to the intramolecular isomerization of the common peroxide linkage intermediate involving the breakage of the C–H bond in the methyl group to the adsorbed hydroperoxide. The latter

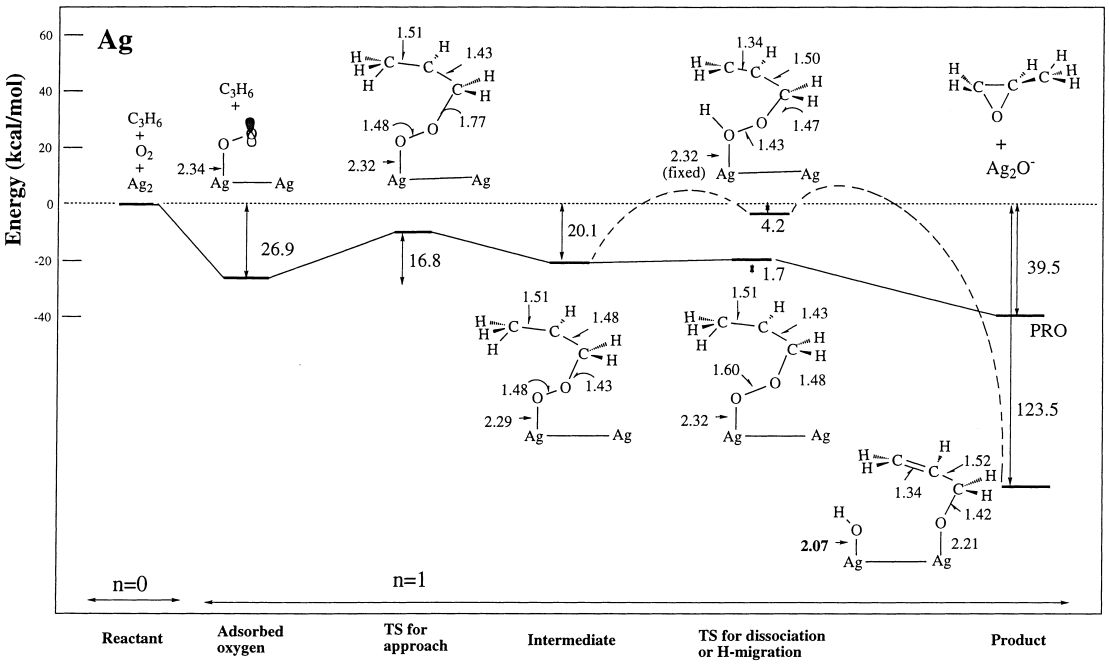

Fig. 14. Energy diagram for the reaction between terminal carbon atom of propylene and molecularly adsorbed superoxide on Ag surface. The route leading to propylene oxide is given by the solid line, and the intramolecular isomerization of methyl hydrogen is shown by the broken line.

would decompose rapidly at the reaction temperature. We have checked this mechanism as it seems to be an attractive model based on the molecularly adsorbed oxygen. Fig. 14 shows the results of our calculation. Propylene approaches the adsorbed superoxide species in a similar way as shown in Fig. 3 but with the methyl group left in the same side as O_a (the inside oxygen atom), which may lead to a possible intramolecular isomerization of one H(γ)–C to the HOa in the next reaction step. However, the energy levels of the TS and intermediate are 16.8 and 20.1 kcal mol^{-1}, which is higher than 13.7 and 28.8 kcal mol^{-1} shown in Fig. 3, showing that this reaction path is less favorable. If the intermediate is formed, the next reaction step leading to propylene oxide is more favorable. However, the energy barrier for the intramolecular isomerization of an allylic hydrogen seems to be much higher, though a reasonable TS geometry could not be calculated. Also, the hydroperoxide species suggested by Cant and Hall [8] may not be a stable adsorbed species.

The mechanism proposed by Carter and Goddard [29] is somewhat similar to that suggested by Cant and Hall [8], though two atomically adsorbed oxygens are considered to be involved as the active species. Unfortunately, it is difficult to checked this mechanism exactly by the present model used. However, our calculations show that the abstraction of the γ-hydrogen by the nearest neighbor oxygen atom as suggested by Carter and Goddard [29] seems to be difficult. The C–H(γ) bond distance in the optimized intermediate state by atomically adsorbed oxygen shown in Fig. 5 is 1.088 Å, which is shorter than the C–H(α) one of 1.098 Å in the same intermediate, showing that the C–H bond in the methyl group of the intermediate is stronger than that of C–H(α) bond. This means that the γ-H of the adsorbed intermediate cannot be easily abstracted, and also that it cannot be transferred via the intramolecular isomerization appearing in Cant and Hall's model [8] discussed above. A similar judgement can be made from bond dissociation energies for hydrocarbons [59]:

the C–H bond in the methyl group of the intermediate involved in the oxidation of propylene is stronger than that in the methylene group of the intermediate involved in the oxidation of ethylene as pointed out by Akimoto et al. [14]. Furthermore, both models [8,29] suggested the alkoxide intermediate, which may be oxidized further to CO_2 and H_2O. The alkoxide intermediate was calculated to be 123.5 kcal mol^{-1} (shown in Fig. 14), more stable than the free reactant state, and if it exists, it should be easily checked out by the infra-red spectroscopic study and acrolein should be one of the products. Though one infrared spectroscopic study [13] seems to support an adsorbed acrolein intermediate, however, as pointed out by Madix et al. [27], additional work is necessary to characterize further this intermediate state. In fact, most of the experimental results [8–11] show that only propylene oxide, CO_2 and H_2O are the products of the oxidation of propylene. This mechanism is also inconsistent with the experimental fact that the epoxidation of norbornene occurs readily, regardless of the oxygen adatom coverage between 0.05 and 0.5 [36] as pointed out by Madix et al. [28]. Therefore, the mechanisms involving a single common precursor intermediate to both epoxidation and complete combustion are less favorable.

The mechanism for the complete oxidation of propylene had been proposed by Madix et al. [28], and an acid–base reaction between atomically adsorbed oxygen and an allylic C–H bond was assumed. The reaction was explained to be controlled by the acidity of the C–H bond, i.e. the heterolytic C–H bond dissociation, not the homolytic dissociation energy. The present results confirm that the dominant mechanism for olefin combustion is the activation of an allylic C–H bond by the adsorbed oxygen, and the anionic adsorbed intermediate is indeed stable on the silver surface which can be naturally considered by the DAM used in this study.

The calculated results presented in Sections 3 and 4 clearly enable us to address the mechanism of the epoxidation reaction as well as that of the complete combustion of propylene: epoxidation reaction is initiated by the attack of the adsorbed oxygen to the C=C double bond. The reaction may be written as:

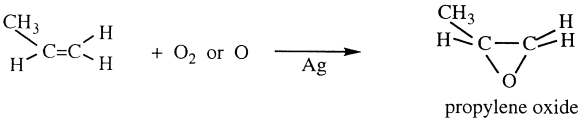

(1)

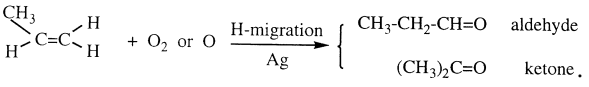

(2)

In Eq. (2), aldehyde is a product of the terminal C attack, ketone is a product of the central C attack, and they are further oxidized to CO_2 and H_2O.

The complete oxidation route is initiated by the abstraction of the allylic hydrogen of propylene by the adsorbed oxygen, and the reaction proceeds as follows:

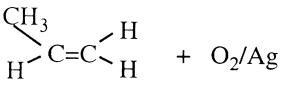

(3)

$$\rightarrow CH_2\text{–}CH\text{–}CH_2/Ag + H\text{–}O\text{–}O/Ag$$

$$\rightarrow CH_2\text{–}CH\text{–}CH_2/Ag + O/Ag + HO/Ag \quad (4)$$

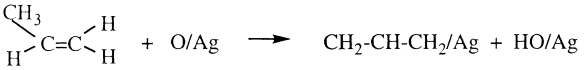

(5)

The allyl intermediate would lie on the surface, therefore being amenable to further attack of adsorbed oxygens and finally oxidized to CO_2 and H_2O.

When allylic hydrogen exists in the olefin, the oxidations (3) and/or (4) would proceed, but when such hydrogen does not exist, the epoxidation reaction (1) would proceed. It is difficult for reaction (2) to proceed for the superoxide species because of the existence of a high energy barrier, but it may proceed partially for the atomically adsorbed species.

6. Conclusion

We studied, in this paper, the mechanism of the epoxidation and complete oxidation reaction of propylene on a silver surface. We performed both the (U)HF and MP2 calculations with the use of the dipped adcluster model (DAM), which involves the interaction between bulk metal and admolecules with consideration of electron transfer and image force correction.

The dominant mechanism for the epoxidation of olefins involves the reaction of the adsorbed oxygen species with the olefinic carbon atom with a formation of a σ bond between the oxygen and the olefinic carbon and with a breaking of the C–C π bond. The further reaction is an easy path that proceeds quite smoothly, leading to an epoxide product. The competitive reaction is complete oxidation via aldehyde intermediate. The molecular superoxide species is the main active species that is selective, but the atomic oxygen species is also active though non-selective.

The dominant mechanism for the complete oxidation of propylene is due to the activation of the allylic C–H bond. The initial step is the abstraction of an allylic hydrogen by the adsorbed oxygen, resulting in the formation of a surface hydroperoxyl [$HOO_{(a)}$] and/or hydroxyl group [$HO_{(a)}$] and a chemisorbed allyl species [$C_3H_{5(a)}$]. The adsorbed surface hydroperoxyl [$HOO_{(a)}$] is further decomposed to an adsorbed hydroxyl group and oxygen atom [$O_{(a)}$] without any difficulty. The adsorbed allyl species is stable for π conjugation and is anionic in nature. It is further combusted to form CO_2 and H_2O in the presence of oxygen. $HO_{(a)}$ can react subsequently with the second hydroxyl via disproportionation to form gaseous water and regenerated $O_{(a)}$ at the reaction temperature. This combustion pathway is more favorable than the epoxidation mechanism for the olefins containing allylic C–H bonds such as propylene studied in this paper.

The above proposed two competitive mechanisms explain rather well the available experimental facts for the epoxidation and complete oxidation of olefins: the olefins contain no allylic C–H bond and/or no subsequent resonance-stabilized allyl radical or anion formation, such as ethylene, styrene, 3,3-dimethylbutene, and norbornene mainly producing epoxide according to the mechanism via the C=C bond breaking, whereas the olefins contain allylic C–H bonds, such as propylene, butenes and pentenes mainly leading to the complete oxidation through the reaction of the allylic hydrogen with the adsorbed oxygen. The DAM was essential for the theoretical study of these reactions.

We note that the present results clearly show that the route leading to propylene oxide also exists on a silver surface. However, it is not the most favorable reaction path. The selectivity is just between 2 and 5% experimentally. Since propylene oxide is an important material in the chemical industry, it is interesting to determine whether we can block the route leading to the allylic intermediate.

Acknowledgements

Some calculations were performed using the computers at the Institute for Molecular Science. Part of this study was supported by a Grant-in-Aid for Scientific Research from the Ministry of Education, Science, and Culture of Japan and by the New Energy and Industrial Technology Development Organization (NEDO).

References

[1] R.A. van Santen, H.P.C. Kuipers, Adv. Catal. 35 (1987) 265.
[2] W.M.H. Sachtler, C. Backx, R.A. van Santen, Cat. Rev. Sci. Eng. 23 (1981) 127.
[3] X.E. Verykios, F.P. Stein, R.W. Coughlin, Cat. Rev. Sci. Eng. 22 (1980) 197.
[4] K.A. Jørgensen, Chem. Rev. 89 (1989) 431.
[5] A. Ayame, in: Y. Murakami (Ed.), Series of Lectures on Catalysis VII, Fundamental Industrial Catalytic Reaction, Catalytic Society of Japan, Tokyo, 1985, pp. 170–185 (in Japanese).
[6] A. Ayame, H. Kanoh, Shokubai 20 (1978) 381.
[7] H. Miura, A. Ayame, H. Kanoh, K. Miyahara, I. Toyoshima, Shinku 25 (1982) 302.
[8] N.W. Cant, W.K. Hall, J. Catal. 52 (1978) 81.
[9] M. Imachi, M. Egashira, R.L. Kuczkowski, N.W. Cant, J. Catal. 70 (1981) 177.

[10] C. Henriques, M.F. Portela, C. Mazzocchia, E. Guglielminotti, in: L. Guczi et al. (Eds.), New Frontiers in Catalysis, Elsevier, Amsterdam, 1993, pp. 1995–1998.
[11] M.F. Portela, C. Henriques, M.J. Pires, L. Ferreira, M. Baerna, Catal. Today 1 (1987) 101.
[12] P.V. Geenen, H.J. Boss, G.T. Pott, J. Catal. 77 (1982) 499.
[13] I.L.C. Freriks, R. Bouwman, P.V. Geenen, J. Catal. 65 (1980) 311.
[14] M. Akimoto, K. Ichikawa, E. Echigoya, J. Catal. 76 (1982) 333.
[15] C.T. Campbell, J. Catal. 94 (1985) 436.
[16] C.T. Campbell, J. Catal. 99 (1986) 28.
[17] C.T. Campbell, M.T. Paffett, Surf. Sci. 139 (1984) 396.
[18] C.T. Campbell, M.T. Paffett, Surf. Sci. 177 (1986) 417.
[19] J. Yang, J. Deng, X. Yuan, S. Zhang, Appl. Catal. A: Gen. 92 (1992) 73.
[20] J. Deng, J. Yang, S. Zhang, X. Yuan, J. Catal. 138 (1992) 395.
[21] Y. Peng, S. Zhang, L. Tang, J. Deng, Catal. Lett. 12 (1992) 307.
[22] E.L. Force, A.T. Bell, J. Catal. 38 (1975) 440.
[23] E.L. Force, A.T. Bell, J. Catal. 40 (1975) 356.
[24] R.B. Grant, R.M. Lambert, J. Catal. 92 (1985) 364.
[25] R.A. Van Santen, C.P.M. De Groot, J. Catal. 98 (1986) 530.
[26] J.T. Gleaves, A.G. Sault, R.J. Madix, J.R. Ebner, J. Catal. 121 (1990) 202.
[27] M.A. Barteau, R.J. Madix, J. Am. Chem. Soc. 105 (1983) 344.
[28] J.T. Roberts, R.J. Madix, W.W. Crew, J. Catal. 141 (1993) 300.
[29] E.A. Carter, W.A. Goddard, III, Surf. Sci. 209 (1989) 243.
[30] P.J. Van den Hoek, E.J. Baerends, R.A. Van Santen, J. Phys. Chem. 93 (1989) 6469.
[31] K.A. Jørgensen, R. Hoffmann, J. Phys. Chem. 94 (1990) 3046.
[32] S. Beran, P. Jiru, B. Wichterlova, R. Zahradnik, Proc. 6th Int. Cobgr. Catal., Vol. 1, 1977, p. 324.
[33] Y. Murakomo, K. Tanaka, Nippon Kagaku Kaishi 11 (1977) 1603.
[34] S. Hawker, C. Mukoid, J.P.S. Badyal, R.M. Lambert, Surf. Sci. 219 (1989) L615.
[35] C. Mukoid, S. Hawker, J.P.S. Badyal, R.M. Lambert, Catal. Lett. 4 (1990) 57.
[36] J.T. Roberts, R.J. Madix, J. Am. Chem. Soc. 110 (1988) 8540.
[37] H. Nakatsuji, J. Chem. Phys. 87 (1987) 4995.
[38] H. Nakatsuji, H. Nakai, Y. Fukunishi, J. Chem. Phys. 95 (1991) 640.
[39] H. Nakatsuji, H. Nakai, Can. J. Chem. 70 (1992) 404.
[40] H. Nakatsuji, H. Nakai, Chem. Phys. Lett. 174 (1990) 283.
[41] H. Nakatsuji, H. Nakai, J. Chem. Phys. 98 (1993) 2423.
[42] H. Nakatsuji, R. Kuwano, H. Morita, H. Nakai, J. Mol. Catal. 82 (1993) 211.
[43] H. Nakatsuji, H. Nakai, K. Ikeda, Y. Yamamoto, Surf. Sci. 384 (1997) 315.
[44] H. Nakatsuji, Z.M. Hu, H. Nakai, K. Ikeda, Surf. Sci. 387 (1997) 328.
[45] H. Nakatsuji, Proc. Surf. Sci. 54 (1996) 1.
[46] H. Nakatsuji, Z.M. Hu, H. Nakai, Int. J. Quantum Chem. 65 (1997) 839.
[47] H. Nakatsuji, K. Takahashi, Z.M. Hu, Chem. Phys. Lett. 277 (1997) 551.
[48] M.J. Frisch, M.H. Gordon, G.W. Trucks, J.B. Foresman, H.B. Schlegel, K. Raghavachari, M.A. Robb, J.S. Binkley, C. Gonzalez, D.J. Defrees, D.J. Fox, R.A. Whiteside, R. Seeger, C.F. Melius, J. Baker, R.L. Martin, J.J.P. Stewart, S. Topol, J. Pople, Gaussian 92, Gaussian, Pittsburgh, PA, 1992.
[49] P.J. Hay, W.R. Wadt, J. Chem. Phys. 82 (1985) 270.
[50] S. Huzinaga, J. Chem. Phys. 42 (1965) 1293.
[51] T.H. Dunning Jr, J. Chem. Phys. 53 (1970) 2823.
[52] T.H. Dunning Jr, P.J. Hay, in: H.F. Schaeffer III (Ed.), Modern Theoretical Chemistry, Vol. 3, Plenum, New York, 1977, p. 10.
[53] S. Huzinaga, J. Andzelm, M. Klobukowski, E. Radzio-Andzelm, Y. Sakai, H. Tatewaki, Gaussian Basis Sets for Molecular Calculations, Physical Science Data, Vol. 16, Elsevier, Amsterdam, 1984, p. 23.
[54] M. Tezuka, Y. Ohkatsu, T. Osa, Bull. Chem. Soc. Japan 48 (1975) 1471.
[55] Y. Moro-oka, P.J. Chung, H. Arakawa, T. Ikawa, Chem. Lett. (Tokyo) (1976) 1293.
[56] J.M. Vohs, B.A. Carney, M.A. Barteau, J. Am. Chem. Soc. 107 (1985) 7841.
[57] B.L. Kugler, R. Kokes, J. Catal. 32 (1974) 170.
[58] J.D. Burrington, C.T. Kartisek, R.K. Grasselli, J. Catal. 69 (1981) 495.
[59] C.R. Noller, Chemistry of Organic Compounds, 3rd ed., Saunders, Philadelphia, PA, 1965.